PROJECT FINAL REPORT:

Cutting costs by locating high production wells: A test of the volcanoseismic approach to finding "blind" resources

FINAL REPORT

By Eylon Shalev Peter E. Malin and Wendy McCausland
Earth and Ocean Sciences, Duke University, Durham, NC 27708-0229

Date - 06/06/02

Prepared for the Geothermal Division, Department of Energy
under Contract No. DE-FG07-00ID13863

SUMMARY

In this Final Report we present and discuss the materials that we are using as a basis for a publication submitted to the Bulletin of the Seismological Society of America on the results of our project. These material are presented in the subsequent pages.

Site Effect Dominated Microearthquake Recordings at Mt. Longonot, Kenya

By
Wendy A. McCausland[1]
Anastasia F. Stroujkova
Silas M. Simiyu[2]
Peter E. Malin

Division of Earth & Ocean Sciences
Duke University
Box 90235
Durham, NC 27708

Abstract. In the summer of 2000, Duke University and the Kenyan power generation company, KenGen, conducted a microearthquake monitoring experiment at Longonot volcano in Kenya. Longonot is one of several major late Quaternary trachyte volcanoes in the Kenya Rift. The study was aimed at developing seismic methods for locating buried hydrothermal areas in the Rift on the basis of their microearthquake activity and wave propagation effects. A comparison of microearthquake records from 4.5 Hz, 2 Hz, and broadband seismometers revealed strong high-frequency site and wave-propagation effects. The lower frequency seismometers were needed to detect and record individual phases. Two-dozen 3-component 2-Hz L22 seismographs and PASSCAL loggers were then distributed around Longonot.

Recordings from this network located one seismically active area on Longonot's southwest flank. The events from this area were emergent, shallow (< 3 km), small ($M \leq 1$), and spatially restricted. Evidently, the hydrothermal system in this area is not currently very extensive or active. To establish the nature of the site effects, the data were analyzed using three spectral techniques that reduce source effects. The data were also compared to a simple forward model. The results show that, in certain frequency ranges, the technique of dividing the horizontal motion by the vertical motion (H/V) to remove the source fails because of non-uniform vertical amplification. Outside these frequencies, the three methods resolve the same, dominant, harmonic frequencies at a given site. In a few cases, the spectra can be fit with forward models containing low velocity surface layers. The analysis suggests that the emergent, low frequency character of the microearthquake signals is due to attenuation and scattering in the near surface ash deposits.

1. Introduction

Between July 10 and September 30, 2000, Duke University and the Kenya Electricity Generating Company, KenGen, conducted a microearthquake monitoring experiment around Longonot volcano located in the Central Kenya Rift (Figure 1). The study was sponsored by the United States Department of Energy geothermal resources program, KenGen, and the Incorporated Research Institutes for Seismology program. Its goal was to find ways of characterizing subsurface the hydrothermal resources in rift areas by studying their associated microearthquakes. The choice of study sites was motivated by the results of recent electrical resistivity surveys conducted by KenGen, which indicated the potential for an active hydrothermal system in the Mt. Longonot area.

The Duke University Seismology group has successfully correlated microearthquakes to the presence and properties of hyrdrothermal systems in other volcanic areas. These areas include Long Valley Caldera, CA (Stroujkova and Malin, 2000), Coso Geothermal Reservoir, CA (Lou and Rial, 1997), and The Geysers, CA (Lou, Shalev, and Malin, 1997). Microearthquakes were used to map out seismotectonics, heat sources, and fractures. They were also used to map crack density through shear-wave splitting tomography (Lou and Rial, 1997; Lou, Shalev and Malin, 1997; Malin and Shalev, 1999).

Mt. Longonot's extrusive deposites are trachytic in composition. Extensive pyroclastics blanket the flanks and area surrounding the volcanic edifice, indicating the interaction of external

fluids with the magmatic system (Scott, 1980; Macdonald, 1994). The present primary surface geothermal manifestations at Longonot are weak fumaroles located along the ring fractures of the pit crater. Some secondary manifestations are associated with the alignment of flank eruption centers and fissures (Scott, 1980; Riaroh and Okoth, 1994).

Simiyu (1999 and 2000) and Simiyu and Keller (2000) conducted seismic studies of the nearby geothermal field at Olkaria, Kenya, about 15 km north of Lonogonot. Microseismicity induced by well discharge and local seismicity (MD<3) were monitored. The background seismicity was continuous at a few events a day, with swarms of higher activity at 4- to 5-day intervals. The locations of the events coincided with local surface faults, and the seismic activity was attributed to the movement of fluids in the geothermal system (Simiyu and Keller, 2000). Seismic tomography was used to map out the geothermal heat source and Poisson's ratio was successfully compared to directly measured reservoir parameters (Simiyu, 2000).

While the nature of the geothermal system at Longonot is much well known, it was initially assumed that its microearthquake investigation could proceed along similar lines as reported in the studies listed above. The data discussed here were collected on a network of twenty-four stations covering an 8-km by 8-km area on the southwest flank of Longonot (Figure 1). This specific area was selected from a larger, 20-km by 30-km reconnaissance area around Mt Longonot and the Olkaria field. The larger area was monitored with a fifty-station network of 3-component Mark Products L28 seismometers and triggered, 250 sps RefTek recorders in the preceding months (McCausland et al., 2000; Shalev et al., 2000).

Prior to the smaller deployment, a seismometer comparison test was conducted at stations L53, T02 and T03 (marked in yellow on Figure 1). At these sites 3-component the 4.5-Hz L28, Mark Products 2-Hz L22, and Guralp GMG30 30-s seismometers were deployed and several microearthquakes recorded with the RefTeks. It was found that the L28 rejected a significant amount of the available low frequency earthquake signal because of its 4.5-Hz roll-off. Instead, the L28 records were dominated by higher-frequency P- and S-wave codas. When compared to the broadband sensor, the L22 seismometer captured most of the low frequency microearthquake signal. This seismometer was also found to be less sensitive to the details of its deployment and the presence of cultural and environmental noise, and was selected for the full deployment with the RefTek recorders.

2. The Longonot Deployment and Earthquake Data Set

Whenever possible the L22 seismometers were installed with plaster-of-Paris to what appeared to be more solid outcrops, with the aim of increasing the signal-to-noise and reducing the effects of poor coupling to the loose surface ash layers. Each station consisted of a 3-component seismometer, a RefTek recorder set to trigger at 250 sps, a GPS clock, and a car battery locked into a buried metal box. A long-term average of 12-s and a short-term average of 0.2-s were used in calculating the trigger ratio.

Although the area around Longonot is remote, it is still subject to a significant amount of cultural noise: foot traffic of Maasai herders and their livestock; noise from passing aircraft; and periodic dynamite blasts from a nearby rock quarry. Many of the stations were located next to homes for security purposes, increasing the likelihood of cultural noise.

A total of 23 locatable earthquakes were recorded in the target area with a minimum of 4 stations giving P and S arrival times (Figure 2). The locations were found using the velocity structure in Table 1. The times and locations of the 17 best events used in the site effects study are listed in Table 2. All these events were small (M<1), shallow (depth ≤ 3-km), and their P- and S-wave arrivals were emergent and had long trailing codas, making it difficult to be certain of their location accuracy. Event location difficulties combined with field observations suggest that the local velocity structure is grossly laterally heterogeneous over the extent of the network. Consequently the location errors are several hundred meters or more in both the horizontal and vertical directions. None of the events were recorded on an adequate number of stations to determine a focal mechanism.

3. Background to the Spectral Analysis for Site versus Source Effects

For all of the spectral analyses, only stations that recorded more than 5 earthquakes were used. These criteria resulted in 13 useful stations and 17 useful events (Table 2). The spectra of these data were used in three different analysis techniques in an effort to understand the factors controlling their appearance. The data were prepared for spectral analysis by correcting the raw signal amplitudes for geometrical spreading.

The raw spectra of these events showed harmonics that could result from either site effects or source processes, or a combination of both. However, the emergent, low frequency, and reverberating character of their seismograms suggested that strong scattering, attenuation, and site effects are present in the subsurface. Further, the harmonics appear site specific (Figure 3) and persistent from event to event (Figure 4).

As discussed by Finn (1991), site response studies are ordinarily a geotechnical engineering concern, and a reference signal is typically used to determine these effects. Good references are the signals at the base of the soil layers or at a neighboring hard rock site (Finn, 1991; Nakamura, 1989). The natural resonant frequency of order n of a loose surface soil layer, assuming weak motion, a uniform elastic layer of thickness, H, and a constant shear wave velocity, is

$$f_n = \frac{(2n-1)\beta}{4H},$$

where n=0 is the fundamental mode. This natural frequency has two independent variables: the layer thickness and the shear wave velocity. When soft surface layers amplify seismic waves, the horizontal amplification is assumed to result primarily from multiply reflected S-waves and the vertical amplification from multiply reflected P-waves. Because of

velocity and wavelength considerations, P-wave amplification in the near surface can generally be ignored. This is especially true if the near surface velocity exceeds 1 km/s and the frequencies are of 10 Hz or less, because then the layer thickness necessary for amplification exceeds tens of meters.

Surface topography can cause signal amplification or damping (Silva, 1991). Of particular importance is the relationship between the lateral dimension of the structure and the wavelength of the incident waves (Finn, 1991). When these two are comparable the signal distortion is severe. Given the surface shear velocities of 1.1 km/s for the ash and 1.6 km/s for the trachyte lava, and 2-30 Hz frequency range, the corresponding wavelengths are 37 – 550 m and 53 – 800 m, respectively. Stations located on or near any structures within these size ranges- lava flows, caldera walls- can be affected.

Given the small number and sizes of the Longonot earthquakes, spectral stacking, or summing, was a good way to begin to examine the case for site related amplifications. The spectrum for each component, station, and event located was normalized by its total energy, thus preventing larger events from dominating the stack. Figure 5 shows stacked velocity spectra for the thirteen stations. Their station dependence suggests that the spectra include significant site effects. Peaks common to several stations correlate with local geological features, as in the cases of stations F01 and F14, which are located on thick ash deposits.

One estimate of the amount of seismic amplification caused by a surface layer can be found by the method of Nakamura (1989). In this method, the site amplification is obtained by dividing the spectrum of a station on soft sediments by the spectrum of a station in a borehole at the base of the sediment layer or a station on solid rock. This site amplification factor or transfer function, A, is therefore defined as

$$A = \frac{H_S}{H_B}, \qquad (1)$$

where HS is the horizontal spectral amplitude at the surface ("S" for surface), and HB is the horizontal spectral amplitude at the base of the layer or a hard rock outcrop ("B" for base or basement).

Nakamura (1989) found from data for different earthquakes at different locations that the ratio of the horizontal (H) to vertical (V) spectral amplitude is close to one for hard soils and rocks. Following this development, and realizing that the vertical component is mostly P-waves that are less affected by the surface layers, Lermo and Chavez-Garcia (1993) modified Nakamura's (1989) ratio so it could be found from the surface vertical component of motion, i.e.:

$$\frac{H_B}{V_B} \cong 1, \text{ so } A \cong \frac{H_S}{V_B}, \text{ and if } \frac{V_S}{V_B} \cong 1, \text{ then } A \cong \frac{H_S}{V_S}, \qquad (2)$$

Examples of this amplification factor for the Longonot events are shown in Figure 6.

While both the spectral stacking and ratio methods give good evidence that site effect dominate the microearthquake signals, they do not give much information about the source. The

inversion method proposed by Andrews (1986) estimates both the site and source effects simultaneously by solving a linear system of equations. The kth observed spectrum, $R_k(f)$, at a given station is assumed to be the convolution of a source term, E, with a site term, S. In the frequency domain:

$$R_k(f) = S_{i(k)}(f) \cdot E_{j(k)}(f), \tag{3}$$

where i(k) is the station number of record k, and j(k) is the event number of record k.

Taking the logarithm of each side of this equation results in a linear set of equations for each frequency, f, of the form,

$$Log(R_k) = Log(S_{i(k)}) + Log(E_{j(k)}). \tag{4}$$

When written in matrix notation, this equation takes the form

$$R = \underline{\underline{IJ}}\,\underline{x} \tag{5}$$

$\underline{\underline{IJ}}$ is an m×n selection matrix of zeroes and ones. The number of rows, m, represents the total number of seismic traces used for the inversion. The number of columns, n, represents the number of events plus stations. The solution, x(f), to this linear system yields both a site effect spectrum for each station and a source spectrum for each earthquake.

The system of equations still contains an undetermined degree of freedom regarding the absolute amplitude of the site effect. The event spectra can be divided by any factor or function and the station spectra multiplied by the same, and still give the same result (Andrews, 1986). For an ideal station on hard rock, the mean site amplification factor should equal one. This a priori information, not explicitly contained in the matrix equation, can be used to help constrain the system of equations through a Lagrange multiplier, □. The system of equations must be solved simultaneously with the constraints to obtain a solution. Following Menke (1984, pp. 55-56), a system of equation (5) subject to the constraint can be rewritten as

$$\begin{bmatrix} \underline{\underline{IJ}}^T & \underline{\underline{F}}^T \\ \underline{\underline{F}} & 0 \end{bmatrix} \begin{bmatrix} x \\ \lambda \end{bmatrix} = \begin{bmatrix} \underline{\underline{IJ}}^T R \\ h \end{bmatrix}, \tag{6}$$

where this constraining spectrum is expressed by h, F is a matrix with zeros everywhere except for the position corresponding to the station being used as a constraint, and $\underline{\underline{IJ}}$T is the transpose of matrix $\underline{\underline{IJ}}$.

The spectrum of station F09, the station with the spectrum most like that of a standard earthquake source, was used to constrain the analysis. This station sits in the middle of the youngest lava flow on Longonot. This flow erupted from a series of six centers along a southwest trending fissure that aligns with a similarly trending fissure on the pit crater floor (Scott 1980). Evidently, this outcrop has deep, solid roots.

4. Results and Discussion

Individual spectra as well as stacks over multiple events at individual stations show that stable peaks persist in the Longonot data (Figures 4 and 5). The presence of the peaks is also evident in the time signals. For instance, Stations F01, F05, and F14 have obvious monochromatic characteristics to their time seismograms (Figure 3). The frequency bands of the peaks are not the same from station to station. If the peaks were a source effect, the same peaks would be seen at each station for a given earthquake. If the source effects were different for each earthquake, then they would drown each other out in the stacks. The more likely alternative is that the ground motion at Longonot is dominated by station specific site effects.

Results from the spectral ratio method are shown as dashed lines in Figure 6. The site effects found by this method agree with the results of the stacks. Station F08 shows a peak at 15 Hz on both horizontal components. Station F10 has a broad peak around 17 Hz, Station F11 at 8-10 Hz, etc. However, the individual spectra and stacks also give evidence that, in some frequency bands, the surface vertical components used to calculate the ratios also suffer from either site effects or P-wave source effects (Figures 4, 5, and 6). The joint separation of source and site effects found by inverting the matrix relation in Eq (6) allows for both these possibilities. The results of this inversion are shown in Figure 6 by the solid lines. The strong site effect peaks that emerge from this method agree in position and magnitude with those seen in the spectra, the stacks and in the ratio method when there is no vertical amplification.

For each method, Stations F01 and F14 show consistent dominant peaks at 10-Hz. Station F05 shows a consistent broad peak between 2.5-7 Hz. These peaks are interpreted to be the products of local geological conditions at the recording sites.

An obvious limitation to the analysis is the amount of data available to process and interpret. The Longonot network was in place for three months and yielded only a total of 23 earthquakes. Ideally thousands of earthquakes are analyzed all at the same set stations, where individual clusters can be examined separately to eliminate differences in path.

As pointed out by Finn (1991), the modified Nakamura method has some weak assumptions. One criticism is that the source is unknown for microtremors. Even though it is assumed that Nakamura's division cancels out the source effect, knowing what the source should look like has its uses; it is important to determining if the source has been truly removed. This difficulty is avoided by using microearthquakes whose frequency content is better understood.

Another problem with the modified Nakamura method important to the signal analyses at Longonot, is the assumption that there is no amplification on the vertical component. Finn (1991) suggests that rather than assuming no vertical amplification, it is better to presume the amplification at the base of the layer (HB/ VB) fluctuates much less than the amplification at the surface (HS/VS). So that even without knowing how much these fluctuations at the base of the layer affect the surface spectral ratios, relative amplifications of a site can be determined.

Finn (1991) and Safak (1991) points out several problems in using spectral ratios to compute site amplification. The obvious problems in the case of the Longonot data are the

amplifications of the vertical components, the sensitivity of the spectral ratio to background noise, and the time variation of the frequency content of the source signal (i.e. emergent P-, S-, and coda-waves). As can be seen from the individual spectra and the stacks, the vertical component at some stations is strongly affected by surface layer amplification, invalidating the basic assumption of the method. Not much can be done to get around this problem at Longonot.

Smoothing the data with different running windows before taking the ratio can reduce the sensitivity issue. This was done both by using stacked data and by smoothing over adjacent frequencies in the stacked spectra.

The Longonot records are difficult to separate into pure P- and S-wave segments, so as a first look just over four seconds of the record beginning with the P-wave was used. Further analysis could break the signal into P-, S- and coda waves, and calculate the site amplification for each phase. Indeed spectrograms of some individual events showed a time-varying nature to the signal. However, for the stations with the most obvious site effects (F01, F05, F14), the monochromatic signal persists throughout the entire record, showing time independence.

In addition to comparing the joint site-and-source inversion solution to the spectral stacking and ratio results, this technique was also checked for internal consistency. One way was by comparing analyses with and without the Lagrange multiplier. As might be expected, these two solutions proved to have the same shape site and source effect spectral curves, but different average levels. With the Lagrange multiplier, the values of the site amplifications were constrained to closer to one, a more realistic site effects compared to unconstrained values.

Another way to assess the overall quality of the inversion was to perform a singular value decomposition (SVD) of the matrix $\overset{IJ}{=}$. The SVD method identifies the parameter and null spaces of the data kernel (Menke, 1984, pp. 119-125). The model resolution matrix indicated that the model parameters are well resolved, and the data resolution matrix indicated that the data are not linearly dependant (Figure 7).

A possible weakness of the joint inversion occurs when other effects are important, such as scattering. In such a case, the results would inadequately resolve the source and site effect for each event. However, this is where having consistent results from the results from the stacks and ratios gives considerable confidence in claiming that the data from Longonot are dominated by near station site effects.

As a further check of the case for site dominated ground motion, forward models of the expected site responses for Stations F11 and F02 were calculated using the reflectivity method (e. g. Aki and Richards, 1980, pp. 393-404). The models were matched to the spectra of event No. 6 of Table 2, assuming this event had a double couple source with a 15 Hz Gaussian wavelet spectrum. The initial velocity models assumed for these sites was that of Simiyu and Keller (2000), modified to better reflect the local conditions shown in Scott's (1980) geology map. By adjusting the layer thickness beneath each site, it was possible to match the observed spectra in the band of the assumed source. The models and observed spectra are shown in Figures 8a and 8b. While far from perfect, the positions of observed and model spectral peaks match well enough to indicate that the case for site dominated motion is reasonable.

6. Conclusions

The first thing that one can conclude from this experiment is that there is not a high level of ambient seismicity at Longonot at this time. Further, the small, shallow events that do occur have their high frequency signals strongly effected by the thick near-surface layer of ash (up to 200m). Evidence for this attenuation is provided by the fact that, despite the density of stations deployed, a significant number of events was picked up by only one or two stations, rather than by many.

A complicating factor in the recording process was the high level of background noise from animal and human foot traffic directly at the sites. Given the equipment used in the field, this requiring higher triggering parameters to reduce false triggers, perhaps at the expense of recording very small emergent events. For security reasons, many stations were placed next to homes, where the human effect is further accentuated. Maasai and their herds of cows and goats, as well as the numerous wild animals that live in the Mt. Longonot National Park, visited even the remotest sites.

Site effect dominance also contributed to the emergent character of the seismic recordings. The results from spectral stacking, the spectral ratios, and joint inversion all lead to this conclusion. There is evidence for strong lateral variation in site conditions, since different sites have vastly different spectral peaks. This is corroborated by the surface geology, as the near surface volcanic layers range from lava flows to pyroclastic deposits and vary observably in thickness across the array.

The frequency dependent site effects of the Longonot seismograms are primarily the result of the loose near-surface ash layers. Trachyte lava layers overlying deeper ash layers and other heterogeneities may also contribute to the observed wave motion. It will be necessary to remove all these effects from the data before any conclusions about the nature of the microearthquake sources beneath Longonot can be drawn. The low ambient background seismicity, which occurs at shallow depths and low magnitudes, also indicates that, at this moment in time, the hydrothermal system at Longonot is much less active than the one at Olkaria.

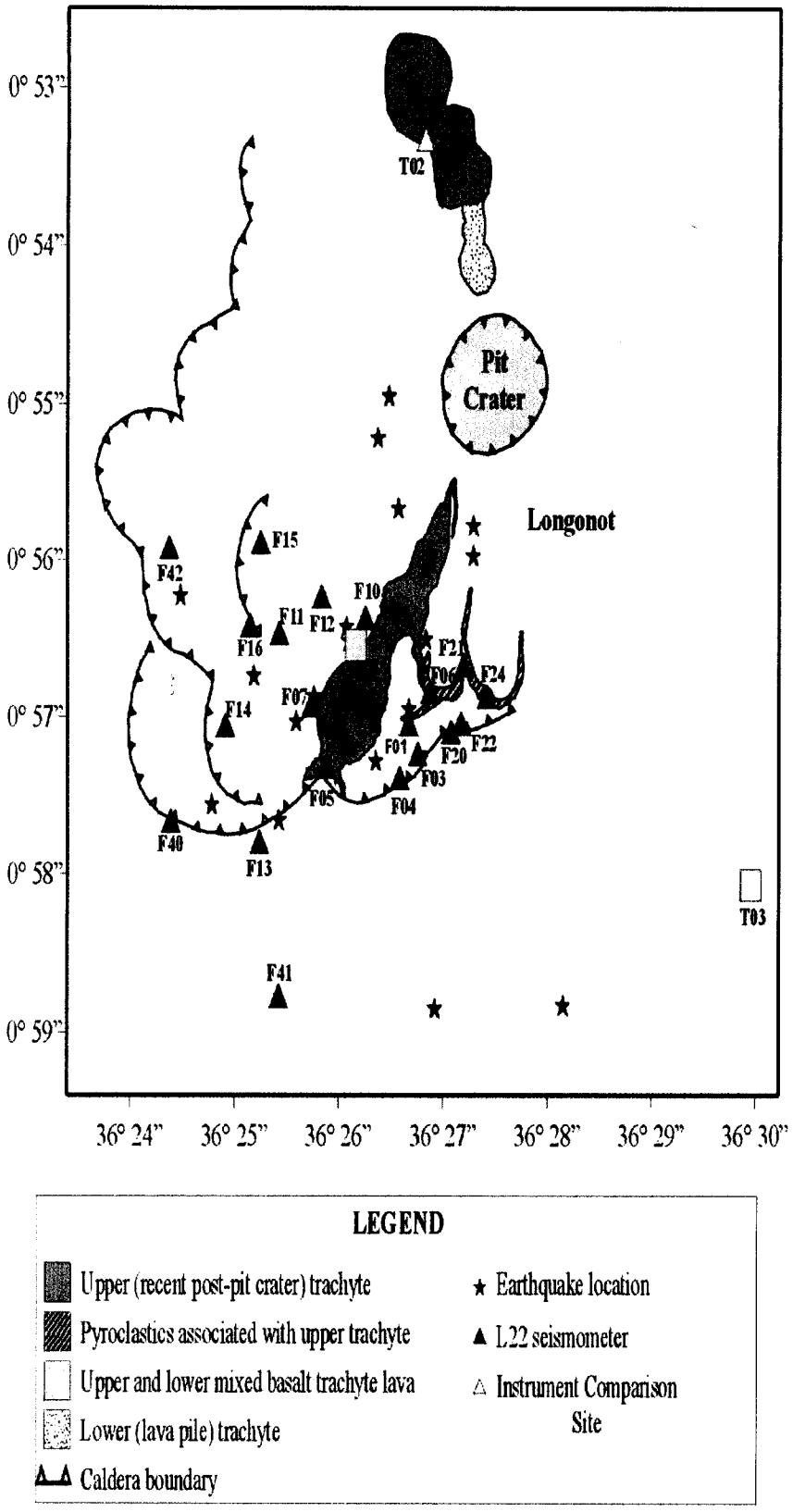

Fig. 1 Station and epicenter locations for Longonot study

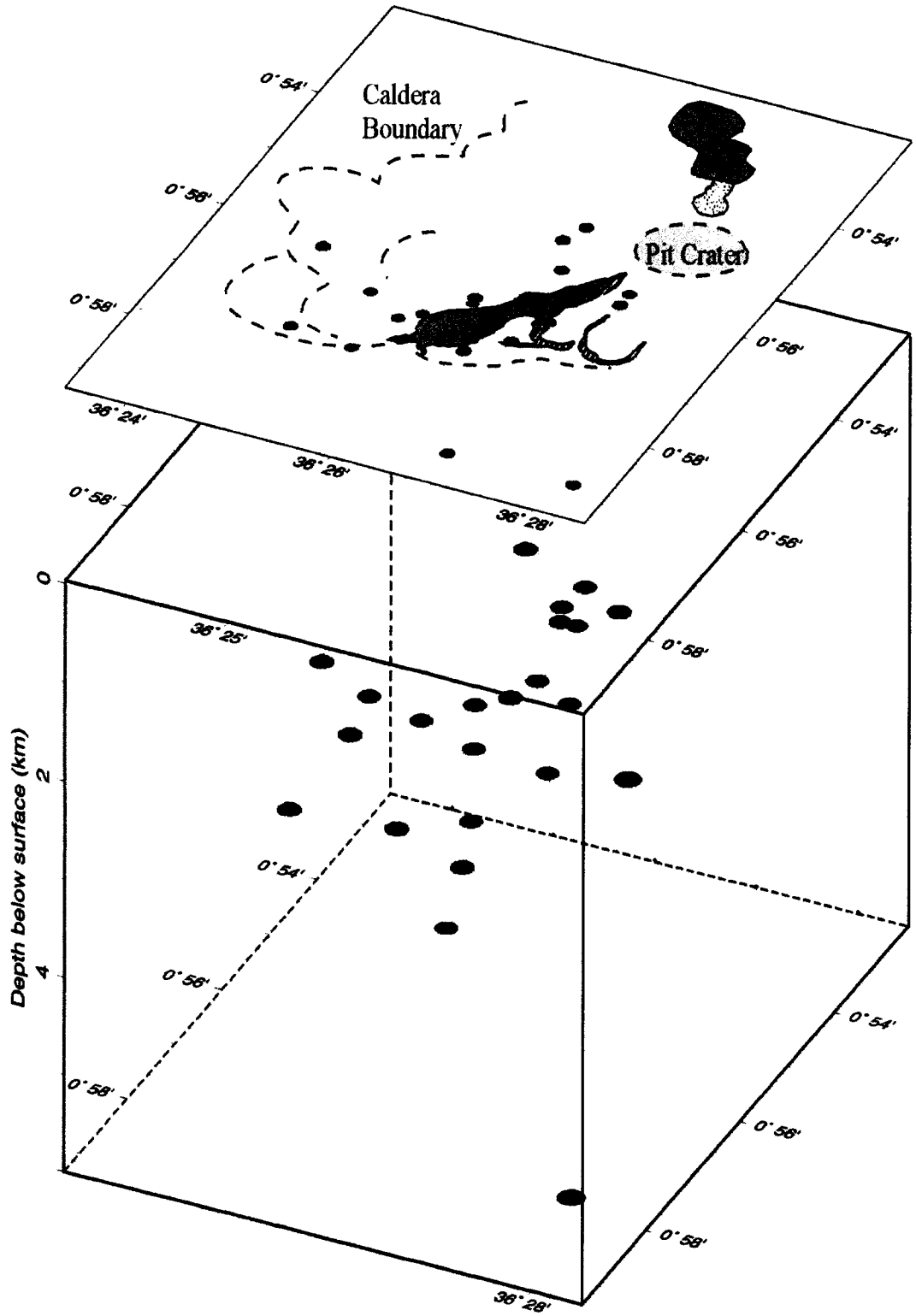

Fig. 2 Block Diagram for July to September 2000 Seismicity

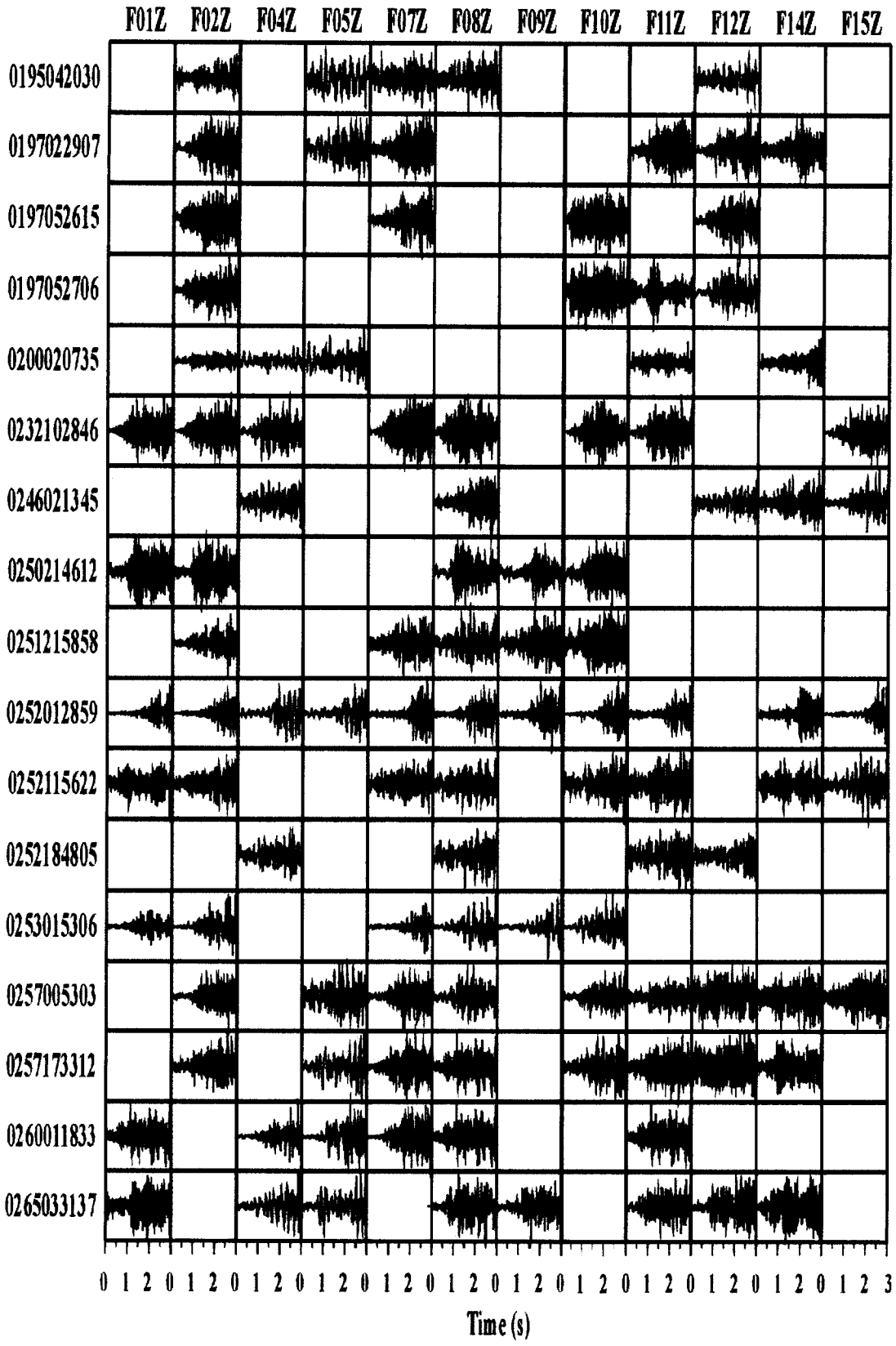

Fig. 3 Vertical Component Seismograms for the 17 earthquakes discussed in the text

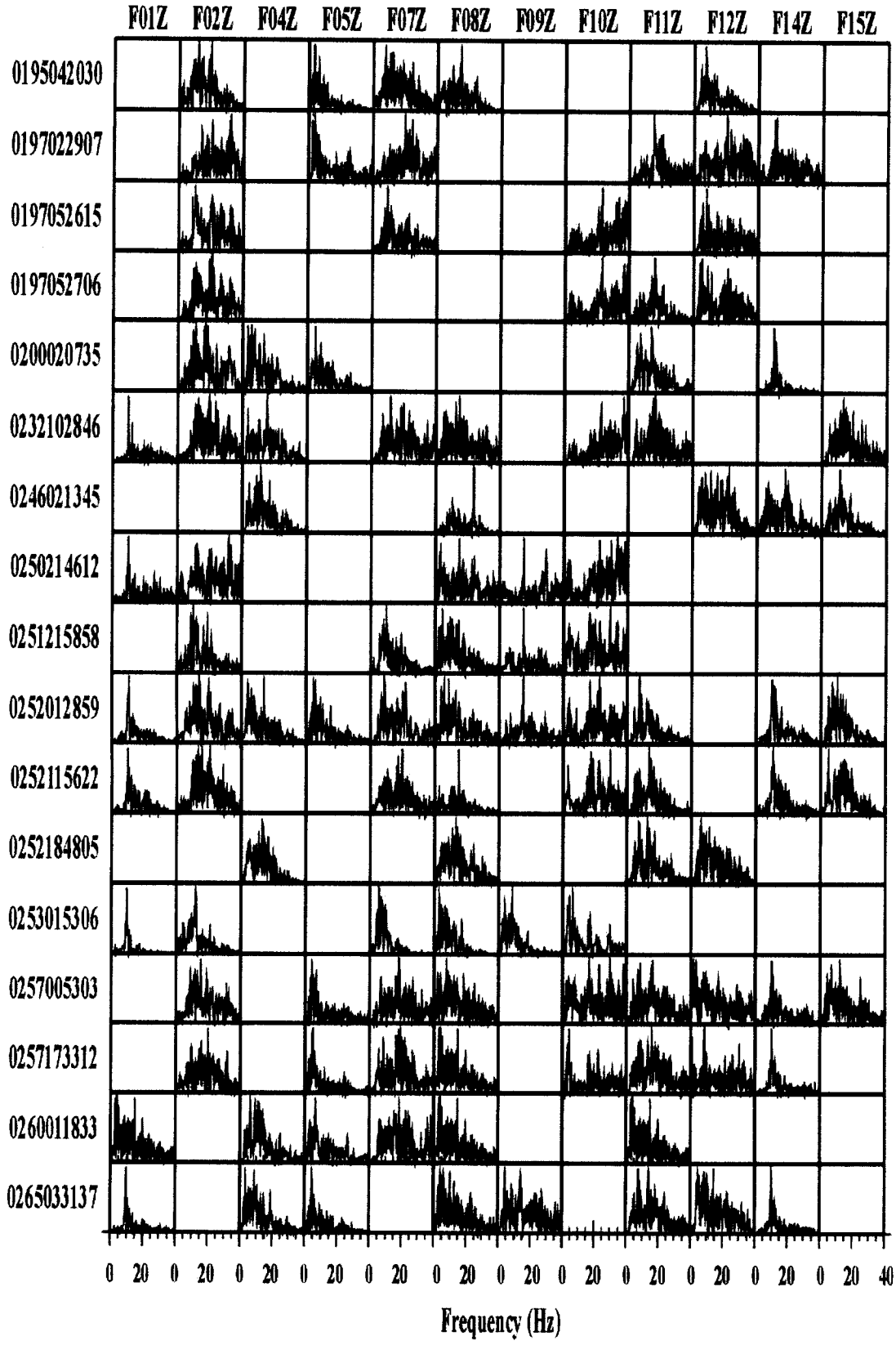

Fig. 4 Vertical Component Velocity Spectra for the Microearthquakes in Figure 3.

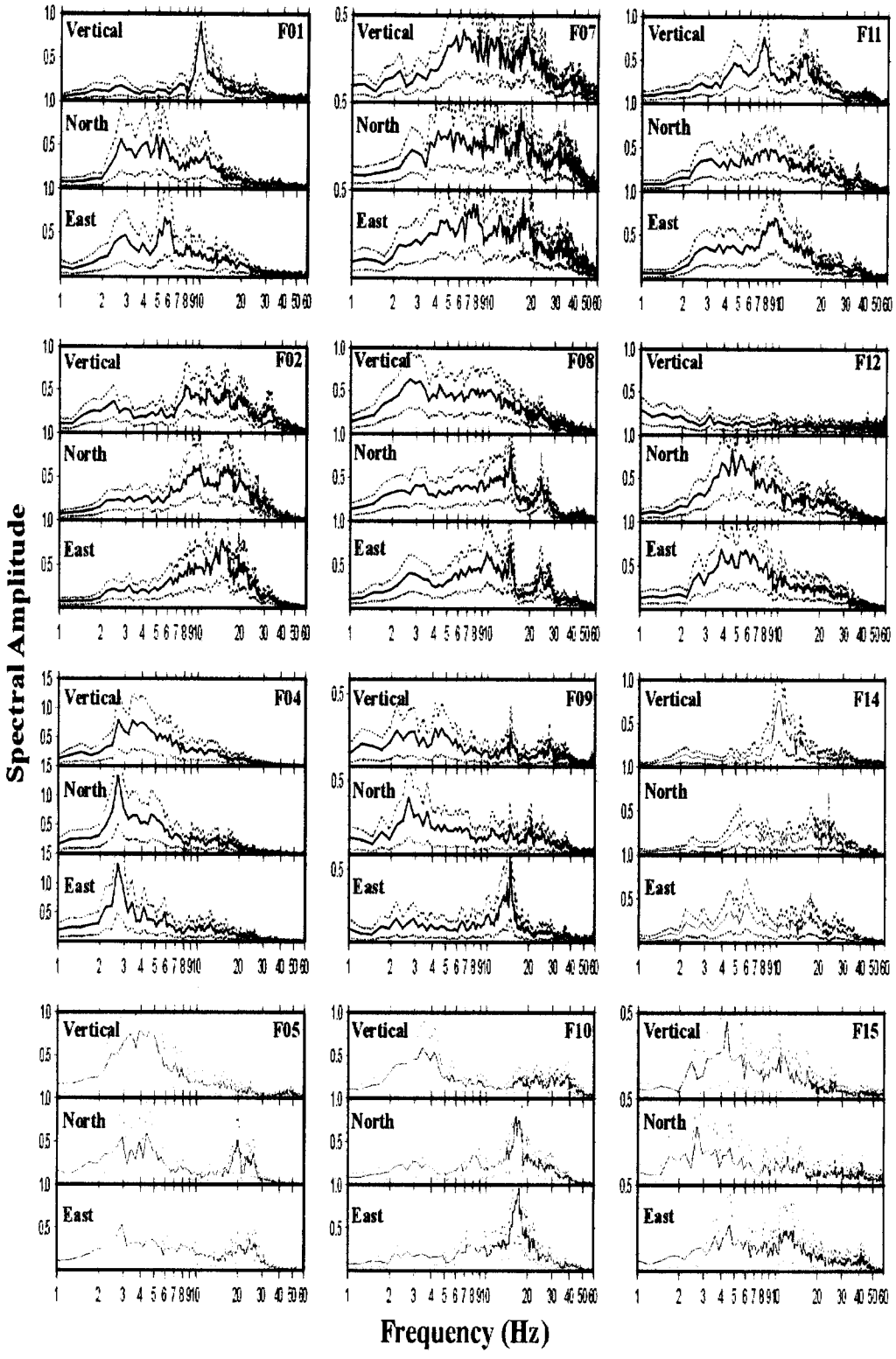

Fig. 5 Energy Normalized Stacks of the 3-Component Spectra

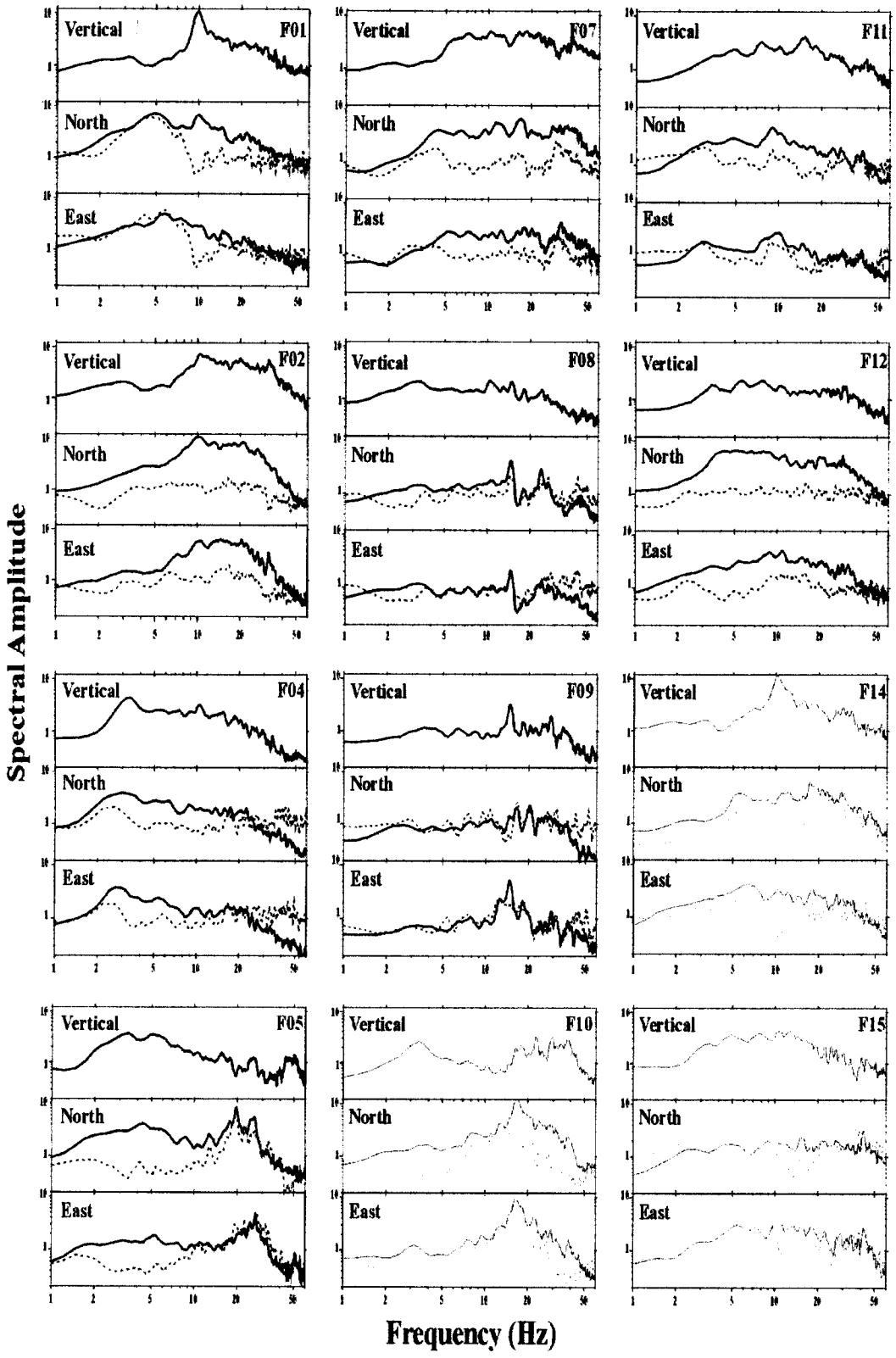

Fig. 6 Comparison of spectral ratios to joint inversion results

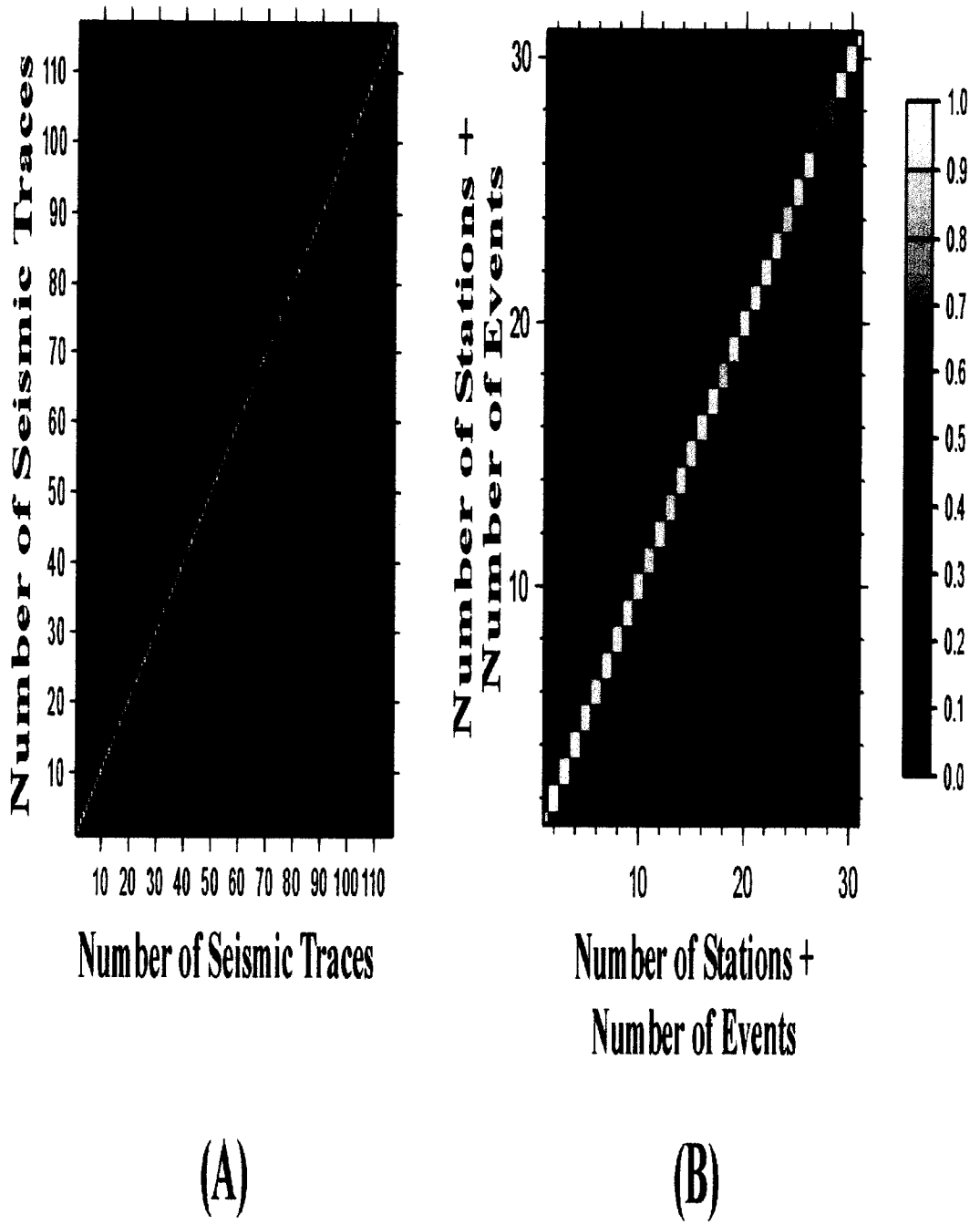

Fig. 7 (A) Data and (B) Model Resolution Matrices for the Joint Inversion.

Fig. 8 a) velocity models for b) models of site effects spectra